MOVEMENT OF A SPHERICAL BROWNIAN PARTICLE BETWEEN INFINITE PARALLEL PLATES: HINDERED DISPERSION AND SEDIMENTATION

by

Ann Terese Heil

Research report submitted in partial fufillment of the requirements for admission to the degree of Master of Science

Department of Chemical Engineering

California Institute of Technology

Pasadena, California 91125

27 May 1988

ACKNOWLEDGEMENTS

My gratitude goes out to a number of people who have helped me in creating this work: my advisor John Brady, for extending technical advice and support; to Lou Durlofsky, for writing the sdwl progams used in my data generation; to John Bauer, for being a friendly and patient system manager on navier; and to Julia, for cheerfully giving many forms of much needed help.

I also extend a warm thank-you to those to helped me on the road to getting to Caltech: Shawn and the rest of the Ann Arbor crew, for being there during my undergraduate years, and my parents, who were my first teachers and who remain my good friends. Finally, I'd like to give a big hug in spirit to all those who have made my life at Caltech a long, strange trip – Erica and Bob, Van, Peter, Jonathan, Tom, Scott, Claudia, Karl, Herma, Mark, Mickey, Jerry, and others too numerous to mention.

ABSTRACT

The dispersion of an isolated, spherical, Brownian particle immersed in a Newtonian fluid between infinite parallel plates is investigated. Expressions are developed for both a 'molecular' contribution to dispersion, which arises from random thermal fluctuations, and a 'convective' contribution, arising when a shear flow is applied between the plates. These expressions are evaluated numerically for all sizes of the particle relative to the bounding plates, and the method of matched asymptotic expansions is used to develop analytical expressions for the dispersion coefficients as a function of particle size to plate spacing ratio for small values of this parameter.

It is shown that both the molecular and convective dispersion coefficients decrease as the size of the particle relative to the bounding plates increase. When the particle is small compared to the plate spacing, the coefficients decrease roughly proportional to the particle size to plate spacing ratio. When the particle closely fills the space between the plates, the molecular dispersion coefficient approaches zero slowly as an inverse logarithmic function of the particle size to plate spacing ratio, and the convective dispersion coefficent approaches zero approximately proportional to the width of the gap between the edges of the sphere and the bounding plates.

TABLE OF CONTENTS

LIST OF FIGURES

1. Introduction

The movement of particles in restricted environments is important in a variety of problems. Particles flowing or diffusing in porous media can be expected to encounter channels of a number of different widths and geometries. In order to fully understand how the particles move, it is necessary to study the behavior of particles in restricted channels of various geometries. Another field in which knowledge of particle movement in restricted environments is important is membrane transport. Membranes may have pores of different geometries - among them cylinders and slits - and transport of mass across the membranes depends on the ability of particles to move through these pores.

In this report we investigate the behavior of particles in restricted environments by examining the behavior of an isolated, spherical, Brownian particle situated in a Newtonian fluid between two infinite parallel plates. We allow the particle to have an arbitrary radius a compared to the spacing between the plates, $2l$, such that $\lambda = a/l$ may vary from nearly zero, corresponding to the plates far from the particle, up to its maximum value of one, corresponding to the plates touching the particle.

We focus our study on the dispersion of a neutrally bouyant particle in a shear flow resulting from relative movement of the plates. The dispersion coefficient is defined in a Lagrangian sense as the steady state limit of the time rate of change of the mean-squared displacement of the particle from its original position. It is also equivalent in an Eulerian framework to the term which relates gradients in particle probability density to probability density flux (Koch and Brady, 1987a). For the situation we are considering, there are two contributions to the dispersion coefficient. The first results solely from 'molecular' diffusion - diffusion in response to random thermal fluctuations - and is present regardless of whether there is a background fluid flow present. If the plates were not present the molecular diffusivity would simply be a scalar constant given by $D_\infty = kT/6\pi\mu a$. However, the plates reduce the ability of the particle to move in response to thermal forces and cause diffusivity to vary as function of position between the walls. Diffusivity is now given by the more general expression, $\mathbf{D} = kT\,\mathbf{M}$, where $\mathbf{M}$ is the hydrodynamic mobility of the particle, and depends on the position of the particle relative to the plates as well as the overall spacing between the plates. The molecular contribution to dispersivity is found by appropriate averaging of diffusivity over the gap between plates. This molecular dispersivity is also related to the average velocity of a non-neutrally bouyant particle settling between two parallel plates, as will be discussed further in Section 2.2.

Convection causes a second contribution to dispersivity which is similiar to Taylor dispersion and is therefore expected to be proportional to Pe^2, where $Pe = Ul/D_\infty$. It arises because the particle mean-squared displacement would grow as t^2 for all times if no molecular diffusion were present, but molecular diffusion slows the spreading and causes the mean-squared displacement to grow linearly with t, resulting in a diffusive process at long times. Note that when the walls are moved to an infinite distance from the particle, the mean-squared displacement of the particle grows as t^3 at long times and the process never becomes diffusive, due to the fact that the particle experiences an ever growing mean-squared velocity with time.

The primary focus of most investigations on restricted diffusion of particles has been on diffusion in circular cylinders. Because hydrodynamic data on particle mobility is needed to calculate the molecular and convective dispersion coefficients, studies have mainly been limited by the availability of this data. One solution has been to use the so-called 'centerline approximation' to obtain molecular dispersivity, in which the molecular dispersivity is taken to simply be the value of molecular diffusivity at the center of the cylinder. Bean (1972) gave an expression for this centerline dispersivity for small λ, good to $O(\lambda^{10})$, where $\lambda = a/R$ and R is the inner radius of the cylinder. Haberman and Sayre (1958), Wang and Skalak (1969), and Paine and Scherr (1975) obtained numerical results for this dispersivity for $0 \leq \lambda \leq 0.9$. Bungay and Brenner (1973) obtained an approximate analytical expression for centerline molecular dispersivity valid for all λ. However, the centerline approximation tends to overpredict the molecular dispersion coefficient because it uses the value of particle diffusivity at the centerline instead of the particle diffusivity averaged over the cylinder radius, and thus does not take into account the sharp drop in particle diffusivity as a particle approaches the walls. Anderson and Quinn (1974) numerically averaged hydrodynamic data for small λ over the cylinder radius to obtain more accurate values for the molecular dispersion coefficient. Brenner and Gaydos (1977) also looked at the limit of small λ, and used the method of matched asymptotic expansions to solve analytically for both the molecular dispersion coefficient and the convective dispersion coefficient in the presence of Poiseuille flow. The limit of a sphere fitting closely into the cylinder, described by $\lambda \approx 1$ or equivalently $\epsilon \ll 1$ where $\epsilon = \lambda^{-1} - 1$, has recently been considered by Mavrovouniotis and Brenner (1987) who calculate only the molecular dispersion coefficient.

Weinbaum (1981) considered dispersion of particles of finite size between infinite parallel plates. He calculated the molecular dispersion coefficient for intermediate values of λ, $0.1 \leq \lambda \leq 0.8$. However, he did not consider the asymptotes of small and closely fitting spheres or the convective dispersion coefficient.

In this report we investigate the dispersion coefficients for a particle between infinite parallel plates for all values of λ. We consider both molecular dispersion and the convective contribution to dispersivity when a background shear flow is present. We begin by developing expressions for the molecular and convective contributions to dispersivity in terms of hydrodynamic properties in Section 2. We also show that the terminal velocity of a non-neutrally bouyant Brownian particle settling between parallel plates is proportional to the molecular dispersion coefficient for a neutrally bouyant particle. In Section 3 we numerically evaluate the expressions for the dispersion coefficients for all values of λ. Exact hydrodynamic results from Ganatos *et al.* (1980*a*, 1980*b*, 1982) are used for this evaluation where available, and hydrodynamic results for other values of λ are obtained using a numerical simulation method based on Stokesian dynamics (Durlofsky, 1986). Matched asymptotic expansions are used to derive analytical expressions for the dispersion coefficients as a function of λ for the limit of a particle small relative to the plate spacing, $\lambda \ll 1$, in Section 4. The limit of a particle fitting closely between the plates, $\epsilon \ll 1$, is examined in Section 5, and conclusions drawn from the results are considered in Section 6.

2. Development of Expressions for Transport Coefficients

2.1 *Dispersion in Shear Flow*

We wish to develop expressions which describe the long time behavior of a neutrally bouyant Brownian sphere between two parallel plates which extend infinitely in the x and z directions and are separated by a distance $2l$ in the y direction. The plates are moving with velocities U and $-U$ respectively in the z direction, generating a shear flow between them. The geometry of the system is pictured in Figure 1. The Reynolds number based on particle size, $Re = \rho U a/\mu$, is taken to be small so that intertial effects on particle movement may be neglected.

We begin by defining the probability density $c(\mathbf{x}, t)$ as the probability that the particle is present at position $\mathbf{x}$ at time t. The probability density may be thought of as a concentration, and is equal to concentration in an equivalent system containing a dilute system of noninteracting particles. The equation of conservation for the probability density is

$$\frac{\partial c}{\partial t} + \nabla \cdot \mathbf{q} = 0, \tag{2.1a}$$

$$\mathbf{q} = \mathbf{v}c = \mathbf{u}c - \mathbf{D} \cdot \nabla c, \tag{2.1b}$$

where $\mathbf{q}$ is the probability density flux, $\mathbf{v}(\mathbf{x})$ is the velocity of the particle when it is centered at position $\mathbf{x}$, and $\mathbf{u}(\mathbf{x})$ is the hydrodynamic velocity of the particle when it is centered at $\mathbf{x}$ - that is, its velocity in the absence of Brownian forces. $\mathbf{D}(\mathbf{x})$ is the diffusivity of a particle centered at $\mathbf{x}$. In an unbounded fluid the diffusivity would simply be a scalar, but it is a second order tensor in this case due to the presence of the restraining walls.

We wish to develop expressions which relate the average probability density flux to the the average gradient in probability density. We start by averaging the conservation equation to obtain

$$\frac{\partial \langle c\rangle}{\partial t} + \nabla \cdot \langle \mathbf{q}\rangle = 0, \tag{2.2a}$$

$$\langle \mathbf{q}\rangle = \langle \mathbf{v}c\rangle = \langle \mathbf{u}\rangle\langle c\rangle + \langle \mathbf{u}'c'\rangle - \langle \mathbf{D}\rangle \cdot \nabla\langle c\rangle - \langle \mathbf{D}\cdot\nabla c'\rangle, \tag{2.2b}$$

where $\mathbf{v}' = \mathbf{v} - \langle \mathbf{u}\rangle$ and $c' = c - \langle c\rangle$. $\langle\ \rangle$ denotes a cross-sectional average over the region of the channel accessible to the particle center

$$\langle h\rangle = \frac{1}{2(l-a)}\int_{-l+a}^{l-a} dy\, h(y). \tag{2.3}$$

Note that at long times we expect truely diffusive behavior, so (2.2) has a solution of the form

$$\langle c(\mathbf{x},t)\rangle = \nabla\langle c\rangle \cdot \mathbf{x} - \langle \mathbf{u}\rangle \cdot \nabla\langle c\rangle t, \tag{2.4}$$

where the average probability density gradient is independent of both time and space (Koch and Brady, 1985).

An expression for the probability disturbance c' is found by substituting the definitions of $\mathbf{v}'$ and c' into (2.1) and using (2.4) to obtain

$$\frac{\partial c'}{\partial t} + \nabla \cdot (\mathbf{v}c') = -\mathbf{v}' \cdot \nabla\langle c\rangle. \tag{2.5}$$

We now define $\mathbf{u}' = \mathbf{u} - \langle \mathbf{u}\rangle = \mathbf{v}' + \mathbf{D}\cdot\nabla$. Substituting this into (2.5) gives

$$\frac{\partial c'}{\partial t} + \nabla \cdot (\mathbf{v}c') = -\mathbf{u}' \cdot \nabla\langle c\rangle, \tag{2.6}$$

where we have used the fact that the gradient of the average probability density only has a component in the z direction, $\nabla\langle c\rangle = (d\langle c\rangle/dz)\,\mathbf{e}_z$. The solution to (2.6) is

$$c'(\mathbf{x},t) = -\int dt_1 \int d\mathbf{x}_1 P(\mathbf{x}-\mathbf{x}_1, t-t_1)\mathbf{u}'(\mathbf{x}_1)\cdot\nabla\langle c\rangle, \tag{2.7a}$$

$$\frac{\partial P}{\partial t} + \nabla \cdot (\mathbf{v}P) = \delta(\mathbf{x}-\mathbf{x}_1)\delta(t-t_1). \tag{2.7b}$$

Because the particle is only free to move in the z direction, the hydrodynamic velocity and velocity disturbance will be vectors in the z direction. Since the bounding plates are taken as infinite in the x and z directions, there will be no variation in hydrodynamic properties in the x and z directions. Thus,

$$\mathbf{u}(\mathbf{x}) = u(y)\mathbf{e}_z \tag{2.8}$$

$$\mathbf{u}'(\mathbf{x}) = u'(y)\mathbf{e}_z \tag{2.9}$$

Also, due to the fact that the sphere/plate system has two mutually perpendicular planes of symmetry, $\mathbf{D}$ can be expressed as

$$\mathbf{D} = D_{||}(y)\mathbf{e}_z\mathbf{e}_z + D_{\perp}(y)\mathbf{e}_y\mathbf{e}_y. \tag{2.10}$$

Therefore, (2.7) simplifies to

$$c'(\mathbf{x},t) = -\int dt_1 \int d\mathbf{x}_1 P(\mathbf{x}-\mathbf{x}_1, t-t_1)u'(y_1)\frac{d\langle c\rangle}{dz}, \tag{2.11a}$$

$$\frac{\partial P}{\partial t} + u(y)\frac{\partial P}{\partial z} - D_{||}(y)\frac{\partial^2 P}{\partial z^2} - \frac{\partial}{\partial y}\left(D_{\perp}(y)\frac{\partial P}{\partial y}\right) = \delta(y-y_1)\delta(z-z_1)\delta(t-t_1). \tag{2.11b}$$

The integrations with respect to z_1 and t_1 in (2.11a) may now be performed, resulting in

$$c' = \int dy_1 \tilde{P}(y-y_1)u'(y_1)\frac{d\langle c\rangle}{dz}, \tag{2.12a}$$

where $\tilde{P}$ is given by

$$-\frac{\partial}{\partial y}\left(D_{\perp}(y)\frac{\partial \tilde{P}}{\partial y}\right) = \delta(y-y_1). \tag{2.12b}$$

Equation (2.12) is simplified by first operating on both sides of (2.12a) to obtain

$$\frac{d}{dy}\left(D_{\perp}(y)\frac{dc'}{dy}\right) = \int dy_1 \frac{\partial}{\partial y}\left(D_{\perp}(y)\frac{\partial \tilde{P}}{\partial y}\right)u'(y_1)\frac{d\langle c\rangle}{dz}, \tag{2.13}$$

then using (2.12b) to obtain an ordinary differential equation for $c'(y)$

$$\frac{d}{dy}\left(D_{\perp}(y)\frac{dc'}{dy}\right) = -u'(y)\frac{d\langle c\rangle}{dz}. \tag{2.14}$$

Integrating (2.14) with the assumption of no flux across the plates gives

$$c'(y) - c'(-l+a) = -\int_{-l+a}^{y} \frac{d\tilde{y}}{D_{\perp}(\tilde{y})} \int_{-l+a}^{\tilde{y}} d\gamma\, u'(\gamma) \frac{d\langle c\rangle}{dz}. \tag{2.15}$$

Since $c' = c'(y)$, the term $\langle \mathbf{D} \cdot \nabla c' \rangle$ in the expression for the average flux, (2.2b), gives a contribution to the average flux in the y direction and thus does not contribute to the average flux in the flow direction. Therefore, the average flux in the flow direction is given from (2.2b) as

$$\langle q \rangle_z = \langle u \rangle \langle c \rangle - \left(\langle D_{\|} \rangle + \langle D \rangle_c \right) \frac{d\langle c \rangle}{dz}, \tag{2.16}$$

$$\langle D \rangle_c \equiv \frac{\langle u'c' \rangle}{d\langle c \rangle / dz}, \tag{2.17}$$

where (2.8), (2.9), and (2.10) were used in obtaining this expression. $\langle D \rangle_c$ is evaluated by substituting (2.15) into (2.17), using the definition of $\langle\ \rangle$, (2.3), and rearranging the limits of integration to obtain

$$\langle D \rangle_c = \frac{1}{2(l-a)} \int_{-l+a}^{l-a} \frac{dy}{D_{\perp}(y)} \left\{ \int_{-l+a}^{y} d\gamma\, u'(\gamma) \right\}^2. \tag{2.18}$$

The terms $\langle u \rangle$, $\langle D_{\|} \rangle$, and $\langle D \rangle_c$ determine the flux in the flow direction in response to an applied probability density gradient. Using the fact that $u(y)$ and $u'(y)$ are odd and $D_{\|}(y)$ and $D_{\perp}(y)$ are even, these may be written in dimensionless form as

$$\langle \hat{u} \rangle = 0, \tag{2.19}$$

$$\langle \hat{D}_{\|} \rangle = \frac{1}{1-\lambda} \int_0^{1-\lambda} d\hat{y}\, \hat{D}_{\|}(\hat{y}), \tag{2.20}$$

$$\langle \hat{D} \rangle_c = \frac{1}{1-\lambda} \int_0^{1-\lambda} \frac{d\hat{y}}{\hat{D}_{\perp}(\hat{y})} \left\{ \int_{\hat{y}}^{1-\lambda} d\gamma\, \hat{u}(\gamma) \right\}^2, \tag{2.21}$$

where $\hat{y} = y/l$, $\hat{u} = u/U$, $\hat{D}_{\|} = D_{\|}/D_{\infty}$, $\hat{D}_{\perp} = D_{\perp}/D_{\infty}$, $\langle \hat{D}_{\|} \rangle = \langle D_{\|} \rangle / D_{\infty}$, and $\langle \hat{D} \rangle_c = \left(\langle D \rangle_c / D_{\infty} \right) Pe^2$.

$\langle u \rangle$ is the average velocity at which the particle moves at long times. For shear flow between plates moving at opposite velocities, $\langle u \rangle$ is zero. The terms $\langle D_{\|} \rangle$

and $\langle D \rangle_c$ are the dispersion coefficients, relating the average flux to the average probability density gradient. $\langle D_{\|} \rangle$ is the 'molecular' contribution to dispersivity, and is simply a cross-sectional average of the diffusivity parallel to the plates. It only depends on the configuration of the plates, and is thus independent of the background flow field. $\langle D \rangle_c$ is the 'convective' contribution to dispersivity. It arises due to spreading of probability density caused by the different velocities of different streamlines, and is of $O(Pe^2)$.

The time needed for these coefficients to reach their long time values is simply the time needed for a particle to sample all possible y positions. Since the particle can only move across streamlines to different y positions by diffusion, the time scale is diffusive and is thus given by L^2/D, where L is the length the particle must diffuse and D is the appropriate diffusion constant. In this case, the particle must diffusive a distance of $O(l - a)$ in order to move to all accessible channel positions. The appropriate diffusion coefficient is $\langle D_{\perp} \rangle$, since the particle is moving perpendicular to walls as it diffuses across the channel. Therefore, the time to reach diffusive behavior is given by $(l - a)^2/\langle D_{\perp} \rangle$. For particles small relative to the plate spacing this is just l^2/D_{∞}, since almost all of the channel is accessible to the particle and the diffusion constant is close to its value in an unbounded fluid. For a particle which closely fills the gap between plates, the diffusion coefficient is $O(\epsilon)$ but the portion of the gap which is accessible to the particle center is also $O(\epsilon)$, so the time needed for the dispersion coefficients to reach their long time value is $O(\epsilon)$.

2.2 *Settling Velocity of Brownian Particles in a Quiescent Fluid*

Next we consider a non-neutrally bouyant Brownian sphere freely falling under the influence of gravity in the z direction in an otherwise quiescent fluid between two plates. The geometry of the system is shown in Figure 2. The plates extend to infinity in the x and z directions and are separated by a distance $2l$ in the y direction. They are also taken to be open-ended at infinity. We wish to develop an expression which describes the average rate at which the particle falls at long times.

In a quiescent fluid, the general relationship between the translational velocity of a particle and the force applied to is

$$\mathbf{u}(\mathbf{x}) = \mathbf{M}(\mathbf{x}) \cdot \mathbf{F}(\mathbf{x}), \tag{2.22}$$

where $\mathbf{x}$ is the position of the center of the particle and $\mathbf{M}(\mathbf{x})$ is the translational hydrodynamic mobility of the particle, related to its diffusivity by

$$\mathbf{M} = \frac{\mathbf{D}}{kT}, \tag{2.23}$$

(In general, the translational velocity also depends on the applied torque, but we assume the particle is torque-free).

For the case of a particle between two infinite parallel plates, the expression for $\mathbf{M}$ is given by

$$\mathbf{M} = \frac{1}{kT}\left[D_{\parallel}(y)\mathbf{e}_z\mathbf{e}_z + D_{\perp}(y)\mathbf{e}_y\mathbf{e}_y\right], \tag{2.24}$$

where (2.10) was used in obtaining this expression. For a sphere falling due to gravity, the applied force on the sphere is only in the z direction, and (2.22) becomes

$$\mathbf{u}(\mathbf{x}) = u(y)\mathbf{e}_z, \tag{2.25a}$$

$$u(y) = M_{\parallel}(y)G, \tag{2.25b}$$

where $G = \frac{4}{3}\pi a^3(\rho_p - \rho_f)\mathrm{g}$ is the magnitude of the force due to gravity, ρ_p and ρ_f are the densities of the particle and fluid, respectively, and g is the magnitude of the acceleration due to gravity.

In the absence of Brownian forces, the particle would stay at a constant position y and fall at a constant velocity $u(y)$. However, Brownian forces cause the particle to move across streamlines as it falls and thus its velocity changes as a function of time. To get the average velocity at which the particle falls, we average (2.25) over the cross section between plates

$$\langle u \rangle_s \equiv \langle u \rangle = G\langle M_{\parallel}\rangle = \frac{G}{kT}\langle D_{\parallel}\rangle. \tag{2.26}$$

Using the definition of the cross-sectional average, (2.3), and the fact that $M_{\|}$ is an even function of y, the expression for $\langle u \rangle_s$ can be written in dimensionless form as

$$\langle \hat{u} \rangle_s \equiv \frac{\langle u \rangle_s}{(GD_\infty/kT)} = \frac{1}{1-\lambda}\int_0^{1-\lambda} d\hat{y}\ \hat{D}_{\|}(\hat{y}). \tag{2.27}$$

Note that as we have defined them, the dimensionless molecular contribution to dispersivity and the dimensionless average setting velcity are equal to each other.

3. Calculation of Transport Coefficients

In order to evaluate the average transport properties, $\langle \hat{D}_{\|} \rangle = \langle \hat{u} \rangle_s$ and $\langle \hat{D} \rangle_c$, it is necessary to know the hydrodynamic properties $\hat{u}(\hat{y})$, $\hat{D}_{\|}(\hat{y})$, and $\hat{D}_{\perp}(\hat{y})$. To be complete, these properties should really be written as function of λ as well - $\hat{u}(\hat{y},\lambda)$, $\hat{D}_{\|}(\hat{y},\lambda)$, and $\hat{D}_{\perp}(\hat{y},\lambda)$ - since they depend on the sphere radius to plate spacing ratio as well as the particle position between the plates.

Hydrodynamic properties were obtained using two methods. For intermediate ranges of λ, $0.1 \le \lambda \le 0.8$, exact values were taken from Ganatos *et al.* (1980*a*, 1980*b*, 1982) who calculated them using a boundary collocation technique. Because the Ganatos *et al.* results were in terms of forces and not diffusivities, they were related to diffusivities by

$$\hat{D}_{\|}(\hat{y}) = \hat{F}_{\|}(\hat{y})^{-1}, \tag{3.1}$$

$$\hat{D}_{\perp}(\hat{y}) = \hat{F}_{\perp}(\hat{y})^{-1}, \tag{3.2}$$

where $\hat{F}_{\|}(\hat{y})$ and $\hat{F}_{\perp}(\hat{y})$ are the forces required to move a torque-free particle parallel and perpendicular to the walls with velocity $\mathcal{U}$, nondimensionalized by the force that would be required if the walls were not present, $6\pi\mu a\mathcal{U}$ (Brenner, 1967).

The other method used was developed by Durlofsky (1986) and is approximate, but may be used over the entire range of λ. It is based on a multiparticle simulation method developed by Bossis and Brady (1984) known as Stokesian dynamics, which is essentially a molecular dynamics- type simulation with hydrodynamic interactions included. Durlofsky applied this simulation technique to the case of bounded shear flow, in which interactions between the walls and the particles must be taken into account. Although the method was developed for application to simulation of multiparticle systems, it generates results which agree quite well with the exact values of Ganatos *et al.* over all the values of λ for which they may be compared. Near the walls the agreement was essentially exact, but the simulation tended to overpredict mobilities in the center region by up to 10%. Details of the simulation method and comparison with exact results for a single sphere may be found in Durlofsky (1986).

The expressions for the molecular and convective dispersivities are given in (2.20) and (2.21). The integrals were evaluated numerically using data from 50 points spaced evenly across the portion of the channel accessible to the particle center. The exact Ganatos *et al.* values were used over the range for which they were available, and the simulation results were used outside of this range. The values of $\langle D_{\|} \rangle$ for $0.1 \leq \lambda \leq 0.8$ were taken from Weinbaum (1981), who used data from Ganatos *et al.* to evaluate them.

The molecular contribution to dispersivity, $\langle \hat{D}_{\|} \rangle$, is shown as a function of λ in Figure 3. For a point particle, corresponding to $\lambda = 0$, the diffusivity is equal to its value in an unbounded fluid, as expected. As λ starts to increase, dispersivity starts to drop off roughly proportional to particle size. As λ is further increased, dispersivity drops off much more slowly. When λ is equal to 0.5, corresponding to the sphere filling half of the gap between the plates, dispersivity has only been reduced to half of its value in an unbounded fluid, and at λ equal to 0.9, corresponding to the sphere filling 90% of the gap, dispersivity is still at about one quarter of its point particle value. As λ approaches its maximum value of one, dispersivity drops to zero logarithmically. Note that since the dimensionless settling velocity of a particle between two plates, $\langle \hat{u} \rangle_s$, is equal to $\langle \hat{D}_{\|} \rangle$, it has the same behavior as described for the molecular dispersivity.

The convective dispersivity, $\langle \hat{D} \rangle_c$, is shown as a function of λ in Figure 4. Because $\langle \hat{D} \rangle_c = 2/15$ in the limit of $\lambda = 0$, $\langle \hat{D} \rangle / (2/15)$ is plotted to allow easier comparison between this limit and the values for nonzero λ. As with the molecular dispersivity, the convective dispersivity drops off roughly proportional to particle size for small λ. For intermediate values of λ, $\langle \hat{D} \rangle_c$ drops off more quickly than $\langle \hat{D}_{\|} \rangle$ as λ is increased. At $\lambda = .5$ the convective dispersivity is about at third of its point particle value, and at $\lambda = 0.9$ it only retains about one twentieth of its point particle value. As λ approaches 1, $\langle \hat{D} \rangle_c$ falls rapidly to zero.

The behavior of the transport coefficients for λ close to zero and λ close to one are examined in more detail in Sections 4 and 5.

4. Asymptote for Particle Radius Small Compared to Plate Spacing

In this section we use the method of matched asymptotic expansions to derive expressions for the transport coefficients as a function of λ for the case where the particle radius is small compared to the spacing between plates, $\lambda \ll 1$. The derivation closely follows that of Brenner and Gaydos (1977) who derived expressions for the transport coefficients of a small particle in Poiseuille flow in a circular cylinder.

The nondimensional expressions for the transport properties to be evaluated are given by (2.20) and (2.21). Note that symmetry considerations allow us to integrate over only half of the gap between plates, which was chosen as the top half ($y > 0$) for convenience. We break this region into two parts: an outer region in the center of the channel far from the plates where both plates affect the particle behavior but the particle radius is small compared to its distance from either one, and an inner region where the particle is close to one plate and its behavior is primarily influenced by the one plate. We define a constant $\hat{y}^*$ such that the outer region is described by $0 \leq \hat{y} < \hat{y}^*$ and the inner region is described by $\hat{y}^* < \hat{y} \leq 1$.

Start by considering $\langle \hat{D}_{\|} \rangle$. The expression for $\langle \hat{D}_{\|} \rangle$, (2.20), can be written as a sum of integrals over the outer and inner regions

$$\langle \hat{D}_{\|} \rangle = I_{\|o} + I_{\|i} = \frac{1}{1-\lambda} \int_0^{\hat{y}^*} d(\hat{y})\, \hat{D}_{\|} \hat{y} + \frac{1}{1-\lambda} \int_{\hat{y}^*}^{1-\lambda} d(\hat{y})\, \hat{D}_{\|} \hat{y}. \tag{4.1}$$

In the outer region, $0 \leq \hat{y} < \hat{y}^*$, the particle's movement is affected by both walls so both must be considered in determining hydrodynamic properties. However, since the particle is far from either wall, it may be taken to be small relative to the spacing between them. The diffusivity is then determined by a methods of reflectin type solution in which it is expressed as a sum of contributions proportional to increasing powers of λ. The result is (Ho and Leal, 1974)

$$\hat{D}_{\|}(\hat{y}) = \hat{F}_{\|}(\hat{y})^{-1} = 1 - \lambda \frac{1}{2} K_{A\|}(\hat{y}) + O(\lambda^2), \tag{4.2}$$

where (3.1) was used to relate force and diffusivity and $K_{A\|}$ is a known function of $\hat{y}$ tabulated by Ho and Leal. Substituting (4.2) into (4.1) and integrating gives

$$I_{\|o} = \frac{1}{1-\lambda}\left[\hat{y}^* - \lambda C_1 + \lambda \frac{9}{16}\ln(1-\hat{y}^*) + o(\lambda)\right], \tag{4.3}$$

where C_1 is a constant defined by

$$C_1 = \int_0^1 d\hat{y}\left[\frac{1}{2}K_{A\|}(\hat{y}) - \frac{9}{16}\frac{1}{(1-\hat{y})}\right] = 0.19, \tag{4.4}$$

which was evaluated numerically using Ho and Leal's data for $K_{A\|}$.

To evaluate the contribution from the inner region, $\hat{y}^* < \hat{y} \leq 1-\lambda$, define a new dimensionless variable $\eta = (l-y)/a = \lambda^{-1}(1-\hat{y})$ which varies from 1 at the plate to λ^{-1} at the channel center. $I_{\|i}$ can be written in terms of this new variable as

$$I_{\|i} = \frac{\lambda}{1-\lambda}\int_1^{\eta^*} d\eta\, \hat{D}_{\|}(\eta), \tag{4.5}$$

where $\eta^* = \lambda^{-1}(1-\hat{y}^*)$. In the inner region, the particle's behavior is dominated by the effect of the wall that it is nearest so the particle may be treated as if it were only next to one wall. Therefore, $\hat{D}_{\|}(\eta)$ is simply given by the one particle solution of Goldman *et al.* Evaluating (4.5) with this solution results in

$$I_{\|i} = \frac{1}{1-\lambda}\left[\lambda C_2 + \lambda\eta^* - \lambda - \frac{9}{16}\ln\eta^* + o(\lambda)\right], \tag{4.6}$$

where C_2 is the constant (Brenner and Gaydos, 1977)

$$C_2 = \int_1^{\infty} d\eta\left[\hat{D}_{\|}(\eta) - \left(1 - \frac{9}{16}\eta^{-1}\right)\right] = 0.0030. \tag{4.7}$$

Summing contributions from the outer and inner regions, (4.3) and (4.6), in (4.1) and expanding $1/(1-\lambda) = 1 + \lambda + O(\lambda^2)$ gives the final result for $\langle \hat{D}_{\|} \rangle$

$$\langle \hat{D}_{\|} \rangle = 1 + \frac{9}{16}\lambda \ln \lambda + \lambda(C_2 - C_1) + o(\lambda). \tag{4.8}$$

Equation (4.8) shows that $\langle \hat{D}_{\|} \rangle$ deviates from its value in an unbounded fluid by an amount proportional to $\lambda \ln \lambda$ for small values of λ. Figure 5 shows a comparison of the asymptote for $\langle \hat{D}_{\|} \rangle$ with the numerically calculated value. (Slight differences between the asymptote and numerical results at very low λ are most likely due to the tendency of the simulation method to overpredict values of diffusivity in the center region of the channel.) The asymptote approximates behavior well up to $\lambda \approx 0.1$, then it deviates from the numerically calculated value. Because the asymptotic expression for $\langle \hat{D}_{\|} \rangle$ is only good to $O(\lambda)$, the onset of deviation at $\lambda \approx 0.1$ is not surprising.

Before we evaluate the convective contribution to dispersivity, $\langle \hat{D} \rangle_c$, it is necessary to determine

$$\int_0^{1-\lambda} d\hat{y}\ \hat{u}(\hat{y}) = \int_0^{\hat{y}^*} d\hat{y}\ \hat{u}(\hat{y}) + \int_{\hat{y}^*}^{1-\lambda} d\hat{y}\ \hat{u}(\hat{y}). \tag{4.9}$$

In the outer region, $\hat{u}$ is given by (Ho and Leal, 1974)

$$\hat{u}(\hat{y}) = \hat{y} + \lambda^3 \frac{5}{18} K_D(\hat{y}), \tag{4.10}$$

where K_D is a known function of $\hat{y}$ tabulated by Ho and Leal. In the inner region $\hat{u}$ is given by (Goldman *et al.*, 1967*b*)

$$\hat{u}(\eta) = 1 - \lambda \eta \mathcal{F}(\eta), \tag{4.11}$$

where $\mathcal{F}(\eta)$ has been calculated by Goldman *et al.* Evaluating (4.9) with (4.10) and (4.11) results in

$$\int_0^{1-\lambda} d\hat{y}\ \hat{u}(\hat{y}) = \frac{(1-\lambda)^2}{2} + \lambda^2 C_3 + o(\lambda^2), \tag{4.12}$$

where C_3 is the constant (Brenner and Gaydos, 1977)

$$C_3 = \int_1^\infty d\eta \; \eta[1 - \mathcal{F}(\eta)] = 0.32. \tag{4.13}$$

Finally, we need to evaluate $\langle \hat{D} \rangle_c$, given by (2.21). Expressing it as sum of integrals over the inner and outer regions gives

$$\langle \hat{D} \rangle_c = I_{co} + I_{ci} = \frac{1}{1-\lambda} \int_0^{\hat{y}^*} \frac{d\hat{y}}{\hat{D}_\perp(\hat{y})} \varsigma(\hat{y})^2 + \frac{1}{1-\lambda} \int_{\hat{y}^*}^{1-\lambda} \frac{d\hat{y}}{\hat{D}_\perp(\hat{y})} \varsigma(\hat{y})^2, \tag{4.14a}$$

$$\varsigma(\hat{y}) = \int_{\hat{y}}^{1-\lambda} d\hat{y} \; \hat{u}(\gamma). \tag{4.14b}$$

Start by considering the outer region. We need expressions for $\varsigma(\hat{y})$ and $1/\hat{D}_\perp(\hat{y})$. If we rewrite $\varsigma(\hat{y})$ as

$$\varsigma(\hat{y}) = -\int_0^{\hat{y}} d\gamma \, \hat{u}(\gamma) + \int_0^{1-\lambda} d\gamma \, \hat{u}(\gamma), \tag{4.15}$$

and use (4.10) and (4.12), we obtain

$$\varsigma(\hat{y}) = \frac{(1-\lambda)^2}{2} + \lambda^2 C_3 - \frac{\hat{y}^2}{2} + o\left(\lambda^2\right). \tag{4.16}$$

$1/\hat{D}_\perp(\hat{y})$ is given by (Ho and Leal, 1974)

$$\frac{1}{\hat{D}_\perp(\hat{y})} = \hat{F}_\perp(\hat{y}) = 1 + \lambda \frac{1}{2} K_{A\perp}(\hat{y}) + o\left(\lambda^3\right), \tag{4.17}$$

where $K_{A\perp}$ is a function tabulated by Ho and Leal. The integral I_{co} can now be evaluated. Begin by breaking it into two parts

$$I_{co} = \frac{1}{1-\lambda} \int_0^1 \frac{d\hat{y}}{\hat{D}_\perp(\hat{y})} \varsigma(\hat{y})^2 - \frac{1}{1-\lambda} \int_{\hat{y}^*}^1 \frac{d\hat{y}}{D_\perp(\hat{y})} \varsigma(\hat{y})^2. \tag{4.18}$$

Since the second integral in this expression is only taken over a region in which $\hat{y}$ is close to 1, $K_{A\perp}$ may be approximated for this integral by its value for $\hat{y}$ close to 1

$$K_{A\perp} \approx \frac{9}{4} \frac{1}{(1-\hat{y})}. \tag{4.19}$$

Using this relation along with (4.16) and (4.17) in (4.18) results in

$$
\begin{aligned}
I_{co} = \frac{1}{1-\lambda}\Bigg[& \frac{2}{15} + \lambda\left(-\frac{2}{3} + \frac{C_4}{4}\right) + \lambda^2\left(\frac{4}{3} + \frac{2}{3}C_3 - C_5\right) \\
& + \lambda^3\left(\frac{1}{3}\eta^{*3} - \frac{7}{16}\eta^{*2}\right) + o\left(\lambda^2\right) + O\left(\lambda^4\eta^{*4}\right)\Bigg] ,
\end{aligned}
\tag{4.20}
$$

where C_4 and C_5 are constants defined by

$$
C_4 = \frac{1}{2}\int_0^1 d\hat{y}\,(1-\hat{y}^2)^2 K_{A\perp}(\hat{y}) = 1.10, \tag{4.21}
$$

$$
C_5 = \frac{1}{2}\int_0^1 d\hat{y}\,(1-\hat{y}^2) K_{A\perp}(\hat{y}) = 1.75, \tag{4.22}
$$

which were evaluated numerically using Ho and Leal's data for $K_{A\perp}$.

Now consider the inner region. We again need expressions for $\varsigma(\hat{y})$ and $1/\hat{D}_\perp(\hat{y})$. Using (4.11) in (4.14b), we obtain to leading order,

$$
\varsigma(\hat{y}) = \lambda^2(\eta-1)^2. \tag{4.23}
$$

The first approximation to $1/\hat{D}_\perp(\hat{y})$ in the inner region is (Brenner, 1961)

$$
\frac{1}{\hat{D}_\perp(\eta)} = 1 + \frac{9}{8}\eta^{-1}. \tag{4.24}
$$

Using (4.23) and (4.24) to evaluate I_{ci} gives

$$
I_{ci} = \frac{\lambda^3}{1-\lambda}\left[\frac{1}{3}\eta^{*3} - \frac{7}{16}\eta^{*2} + O\left(\eta^*\right)\right]. \tag{4.25}
$$

Finally, summing the contributions from the inner and outer regions, (4.18) and (4.25), in (4.14) and expanding $1/(1-\lambda) = 1 + \lambda + \lambda^2 + O(\lambda^3)$ gives

$$
\frac{\langle\hat{D}\rangle_c}{2/15} = 1 + \lambda\left(-4 + \frac{15}{8}C_4\right) + \lambda^2\left(6 + 5C_3 + \frac{15}{8}C_4 - \frac{15}{2}C_5\right) + o\left(\lambda^2\right). \tag{4.26}
$$

Equation (4.26) predicts that dispersivity will take on a value of $2/15$ in the limit of the particle size small compared to the plate spacing. It will deviate from this value by an amount proportional to λ for small values of λ. The asymptote for

$\langle \hat{D} \rangle_c$ is compared to the exact solution in Figure 6. The values for the asymptote and the numerical values start to deviate for $\lambda > 0.05$. Because the error in the expression for $\langle \hat{D} \rangle_c$ should be of $o\left(\lambda^2\right)$, the two values should match for greater values of λ. Because the initial slope of the asymptote matches the numerical values, the $O(\lambda)$ term appears to be correct so the problem most likely lies with the $O(\lambda^2)$ term.

Finally, we consider the contribution of excluded volume effects to the convective dispersion coefficient. Excluded volume effects arise due to the finite size of the particle - because the particle has a finite radius, the center of the particle can not move to positions less than one particle radius from the wall. Since the highest velocities are closest to the wall, this effect lowers spreading by convection and thus reduces the convective dispersion coefficient. The effect of the excluded volume is seen by evaluating the expression for $\langle \hat{D} \rangle_c$, (2.21), using the point particle approximation for hydrodynamic properties $\hat{u}(\hat{y})$, $\hat{D}_{\|}(\hat{y})$, and $\hat{D}_{\perp}(\hat{y})$, but not integrating over the region from which the particle center is excluded. This results in

$$\frac{\langle \hat{D} \rangle_c}{2/15} = 1 - 3\lambda + 6\lambda^2 + o(\lambda^3). \tag{4.27}$$

Comparison of (4.26) and (4.27) shows that the excluded volume effect gives a significant contribution to the deviation of the convective dispersion coefficient from its value for a point particle.

5. Asymptote for Particle Size Close to Plate Spacing

Next we consider the case in which the sphere fits closely between the plates, described by $\lambda \approx 1$ or equivalently $\epsilon = \lambda^{-1} \ll 1$. In this case the gap between the sphere and the plate is small, so it is convenient to define a new dimensionless lenth scale, $Y = y/(l - a)$. Y is now an $O(1)$ variable, which ranges from -1 as the sphere touches the bottom plate to 1 as the sphere touches the top plate.

We first consider the molecular contribution to dispersivity. The force required to move a sphere parallel to a single plane wall grows as $O(\ln \sigma) + O(1)$ as σ, the separation between the sphere and the wall nondimensionalized by the particle radius, gets small. Since the logarithmic singularity grows so slowly, the $O(1)$ contribution to force is significant at all but very small values of σ, corresponding to the particle just about touching the wall. When two walls are present and $\epsilon \ll 1$, the sphere is close to both walls at all times. Therefore we expect a contribution to the force required to move the sphere of $O(\ln\sigma) + O(1)$ from each side of the sphere. The logarithmic singularity terms from each side of the sphere are expected to be simply additive, since they come from lubrication forces between the sphere and do not depend on the flow field outside of the lubrication layer. However, the $O(1)$ terms will not be additive because they arise from the flow field outside of the lubrication layer, which will be different for a particle between two walls as opposed to a particle alone next to one wall. Therefore, we expect

$$\hat{F}_{\|}(Y) = \frac{1}{\hat{D}_{\|}(Y)} \approx G_1(\epsilon) + \frac{1}{2}\left[\ln\epsilon(1-Y) + \ln\epsilon(1+Y)\right], \tag{5.1}$$

where G_1 is a function only of ϵ and the $1/2$ arises from the solution for a single particle near a wall (Goldman *et al.*, 1967*a*).

When the expression for $\langle\hat{D}_{\|}\rangle$, (2.20), is written in terms of the rescaled variable Y, it becomes

$$\langle\hat{D}_{\|}\rangle = \int_0^1 dY\, \hat{D}_{\|}(Y). \tag{5.2}$$

Subtituting (5.1) into (5.2) suggests that

$$\langle\hat{D}_{\|}\rangle \approx \frac{1}{K_1 + K_2\ln\epsilon}, \tag{5.3}$$

where K_1 and K_2 are $O(1)$ constants.

Numerical simulation was used to calculate values for $\langle\hat{D}_{\|}\rangle$ for small ϵ. The simulation uses lubrication theory to correctly calculate the singularity at each wall. The method it uses to determine the $O(1)$ term is approximate, but it gives good agreement with exact results over the the range $0.1 \leq \lambda \leq 0.8$ where they can be compared, and should be expected to give good results for λ close to 1. Thus, we expect the simulation to give values for diffusivity which are approximately correct for small ϵ. Figure 7 shows a plot of these values, in the form of $1/\langle\hat{D}_{\|}\rangle$

versus $-\ln\epsilon$. The figure shows that a straight line is obtained, confirming that the form of (5.3) is correct. The constants K_1 and K_2 were found using the simulation results to be $K_1 = 1.2$ and $K_2 = -1.0$.

Now consider the convective contribution to dispersivity. In terms of the rescaled variable Y, the expression for $\langle\hat{D}\rangle_c$ is

$$\langle\hat{D}\rangle_c = \lambda^2\epsilon^2 \int_0^1 \frac{dY}{\hat{D}_\perp(Y)} \left\{ \int_Y^1 d\tilde{Y}\, \hat{u}(\tilde{Y}) \right\}^2. \tag{5.4}$$

For a sphere near a single wall, the force required to move the sphere perpendicular to the wall increases as the inverse of distance from the wall and becomes singular as the sphere touches the wall. For a sphere between two walls we expect a contribution from both walls which should be simply additive, giving

$$\hat{F}_\perp(Y) = \frac{1}{\hat{D}_\perp(Y)} = \frac{1}{\epsilon}\left[\frac{1}{(1-Y)} + \frac{1}{(1+Y)}\right]. \tag{5.5}$$

Substituting this into (5.4) results in

$$\langle\hat{D}\rangle_c = \lambda^2\epsilon \int_0^1 dY \left[\frac{1}{(1-Y)} + \frac{1}{(1-Y)}\right] \left\{ \int_Y^1 \hat{u}(\tilde{Y}) d\tilde{Y} \right\}^2. \tag{5.6}$$

Since $\lambda \approx 1$, this suggests roughly an ϵ scaling of $\langle\hat{D}\rangle_c$ for small ϵ. However, $\hat{u}(Y)$ depends on ϵ, and for small ϵ it exhibits a logarithmic approach to the wall velocity as the sphere nears the wall,

$$\hat{u}(Y) \approx 1 - \frac{1}{H_1(\epsilon) - H_2(\epsilon)\ln\epsilon(1-Y)}, \tag{5.7}$$

Where H_1 and H_2 are functions only of ϵ. Therefore,

$$\langle\hat{D}\rangle_c = \lambda^2\epsilon f(\epsilon) \approx \epsilon f(\epsilon), \tag{5.8}$$

where $f(\epsilon)$ is an unknown logartihmic function. Numerical simulation was used to evaluate $f(\epsilon)$ for small ϵ. Figure 8 gives a plot of $f(\epsilon)$ versus $-1/\ln\epsilon$, showing that $f(\epsilon)$ is roughly proportional to $1/\ln\epsilon$ and suggesting that

$$\langle\hat{D}\rangle_c \sim \frac{\epsilon}{\ln\epsilon}. \tag{5.9}$$

6. Conclusions

As expected, both the molecular and convective dispersion coefficients decrease as λ increases. In the limit of small λ, corresponding to the particle small compared to the plate spacing, the molecular dispersion coefficient is given by $\langle D_{\|}\rangle = D_{\infty}\left[1+\frac{9}{16}\lambda\ln\lambda+\lambda(C_2-C_1)+o(\lambda)\right]$. The first deviations of the coefficient from the point particle value of D_{∞} are thus proportional to $\lambda\ln\lambda$. The convective dispersion coefficient in this limit is given by $\langle D\rangle_c = Pe^2 D_{\infty}[\frac{2}{15} + \lambda\left(-\frac{8}{15}+4C_4\right)+\lambda^2\left(\frac{4}{5}+\frac{2}{3}C_3+\frac{C_4}{4}-C_5\right)+o\left(\lambda^2\right)]$, and thus the first deviations of this coefficient from its point particle value are proportional to λ. Excluded volume effects play a large role in the deviation of the convective dispersion coefficient from its point particle value at small λ.

For the limiting case of λ approaching unity, corresponding to the particle fitting closely between the plates, the molecular dispersion coefficient approaches zero as $\langle D_{\|}\rangle \approx D_{\infty}[1/(K_1+K_2\ln\epsilon)]$, where $K_1 = 1.2$ and $K_2 = -1.0$. This logarithmic decay is quite slow - for $\lambda = 0.995$, the molecular dispersion coefficient still retains about 15% of its value for a point particle. The convective dispersin coefficient approaches zero as $\langle D\rangle_c \sim Pe^2 D_{\infty}(\epsilon/\ln\epsilon)$. This is a more rapid approach to zero than for the molecular dispersion coefficient - for $\lambda = 0.9995$, it has been reduced to about a tenth of a percent of its point particle value.

REFERENCES

Anderson, J.L. & Quinn, J.A. 1974 Restricted transport in small pores. A model for steric exclusion and hindered particle motion. *Biophys. J.* **14**, 130.

Bean, C.P. The physics of porous membranes - neutral pores. *Membranes* G. Eisenman, ed., Dekker, New York. **1**, 1.

Brenner, H. 1961 The slow motion of a sphere through a viscous fluid towards a plane surface. *Chem. Eng. Sci.* **16**, 242-251.

Brenner, H. 1967 Coupling between the translational and rotational brownian motions of rigid particles of arbitrary shape. II. General theory. *J. Colloid Interface Sci.* **23**, 407-436.

Brenner, H. & Gaydos L.J. 1977 The constrained brownain movement of spherical particles in cylindrical pores of comparable radius. *J. Colloid Interface Sci.* **58**, 312-356.

Bungay, P.M. & Brenner, H. The motion of a closely fitting sphere in a fluid-filled tube. *Int. J. Multiph. Flow* **1**, 25-56.

Durlofsky, L. 1986 Topics in fluid mechanics: I. Flow between finite rotating disks. II.Simulation of hydrodynamically interacting particles in Stokes flow. Ph.D. Thesis, Massachusetts Institute of Technology.

Ganatos, P., Weinbaum, S. & Pfeffer, R. 1980*a* A strong interaction theory for the creeping motion of a sphere between plane parallel boundaries. Part 1. Perpendicular motion. *J. Fluid Mech.* **99**, 739-753.

Ganatos, P., Pfeffer, R. & Weinbaum, S. 1980*b* A strong interaction theory for the creeping motion of a sphere between plane parallel boundaries. Part 2. Parallel motion. *J. Fluid Mech.* **99**, 755-783

Ganatos, P., Weinbaum, S. & Pfeffer, R. 1982 Gravitational and zero-drag motion of a sphere of arbitrary size in an inclined channel at low Reynolds number. *J. Fluid Mech.* **124**, 27-43.

Goldman, A.J., Cox, R.G. & Brenner, H. 1967*a* Slow viscous motion of a sphere parallel to a plane wall I. Motion through a quiescent fluid. *Chem. Eng. Sci.* **22**, 637-651.

Goldman, A.J., Cox, R.G. & Brenner, H. 1967*b* Slow viscous motion of a sphere parallel to a plane wall II. Couette flow. *Chem. Eng. Sci.* **22**, 653-660.

Haberman, W.L. & Sayre, R.M. 1958 Motion of rigid and fluid spheres in stationay and moving liquids inside cylindrical tubes. David W. Taylor Model Basin Report No. 1143, U.S. Dept. of Navy, Washington, D.C.

Ho, B.P. & Leal, L.G. 1974 Inertial migration of rigid spheres in two-dimensional unidirectional flows. *J. Fluid Mech.* **65**, 365-400.

Koch, D.L. & Brady, J.B. 1985 Dispersion in fixed beds. *J. Fluid Mech.* **154**, 399-427.

Koch, D.L. & Brady, J.B. 1987*a* The symmetry properties of the effective diffusivity tensor in anisotropic porous media. *Phys. Fluids* **30**, 642-650.

Koch, D.L. & Brady, J.B. 1987*b* A non-local description of advection-diffusion with application to dispersion in porous media. *J. Fluid Mech.* **180**, 387-403.

Mavrovouniotis, G.M. 1986 Hindered sedimentation and dispersion coefficients for rigid, closely fitting brownian spheres in circular cylindrical pores containing quiescent fluids. *AIChE Annual Meet.* Paper No. 85b.

Paine, P.L. & Scherr, P. 1975 Drag coefficients for the movement of rigid spheres through liquid-filled cylindrical pores. *Biophys. J.* **12**, 990.

Wang, H. & Skalak, R. 1969 Viscous flow in a cylindrical tube containing a line of spherical particles. *J. Fluid Mech.* **38**, 75.

Weinbaum, S. 1981 Strong interaction theory for particle motion through pores and near boundaries in biological flows at low Reynolds number. *Lect. Math. Life Sci.* **14**, 119-192.

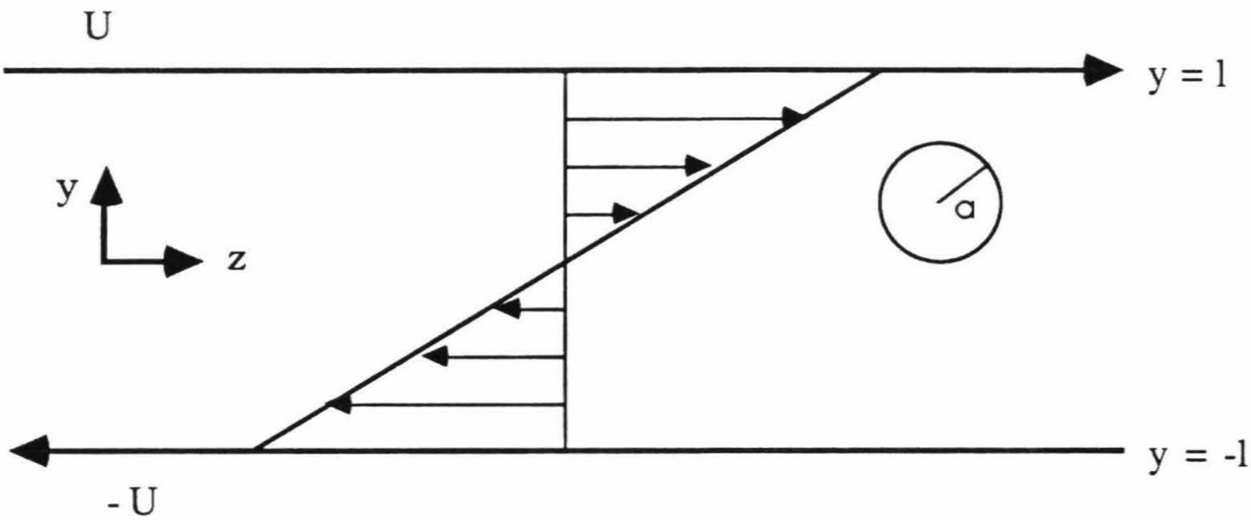

Figure 1. Schematic diagram of a neutrally bouyant spherical particle in shear flow between infinite parallel plates. The planes are infinite in the x and z directions and flow is in the z direction. Sphere centers lie in the $y-z$ plane.

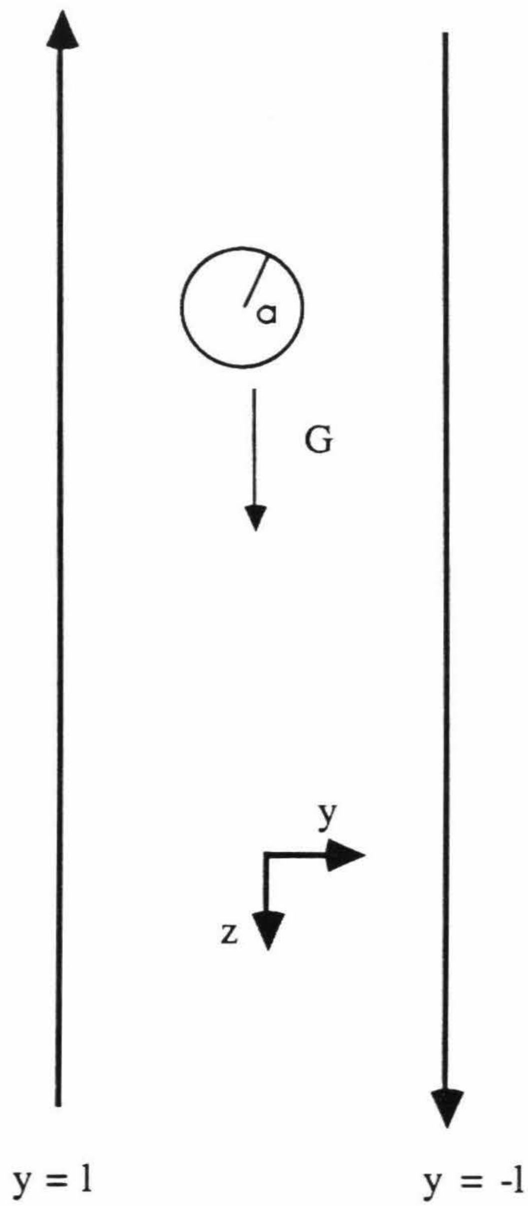

Figure 2. Schematic diagram of a non-neutrally bouyant particle settling due to gravity between infinite parallel plates. The planes are infinite in the x and z directions and flow is in the z direction. Sphere centers lie in the $y-z$ plane.

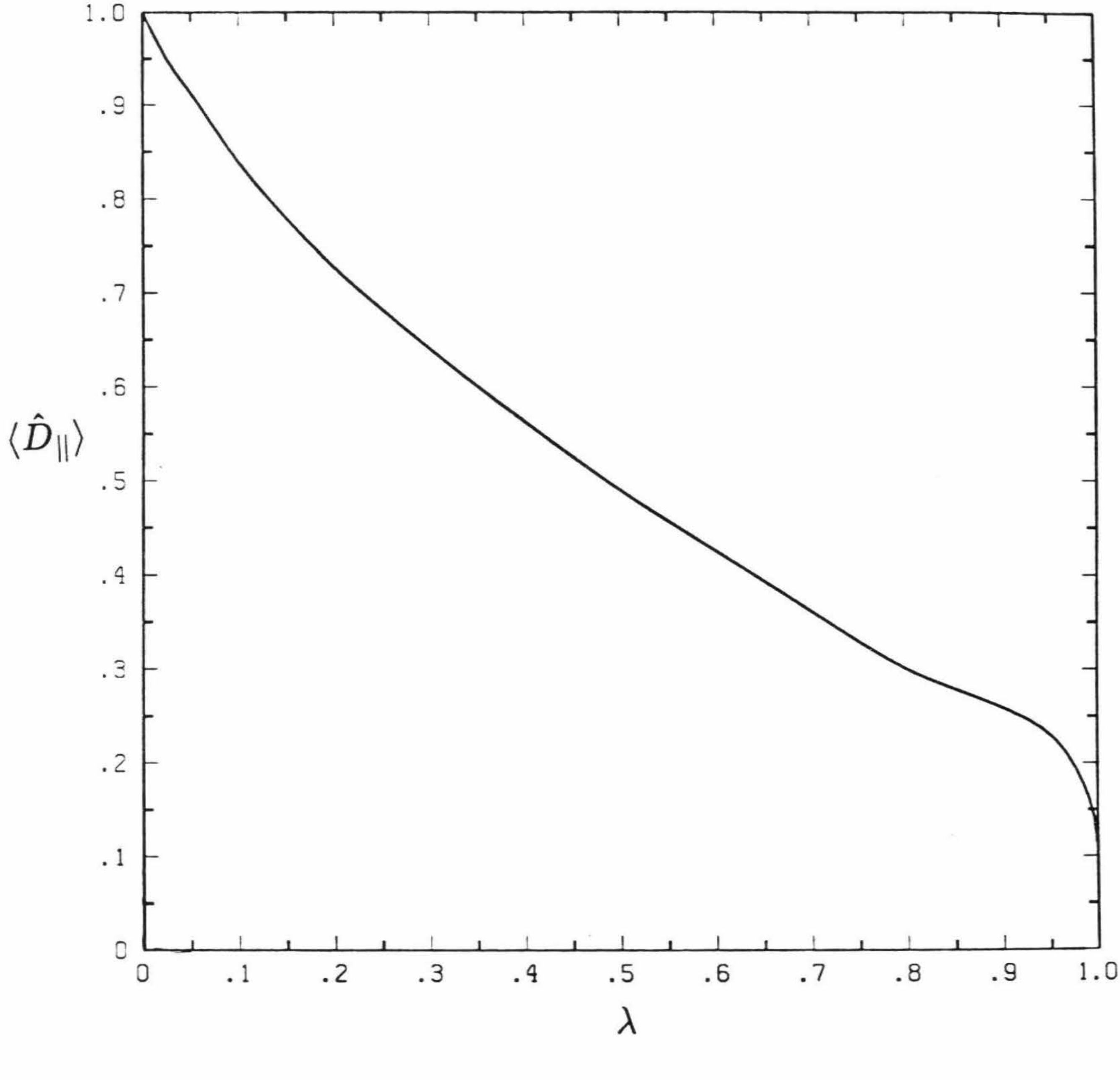

Figure 3. Effect of λ on molecular dispersion coefficient.

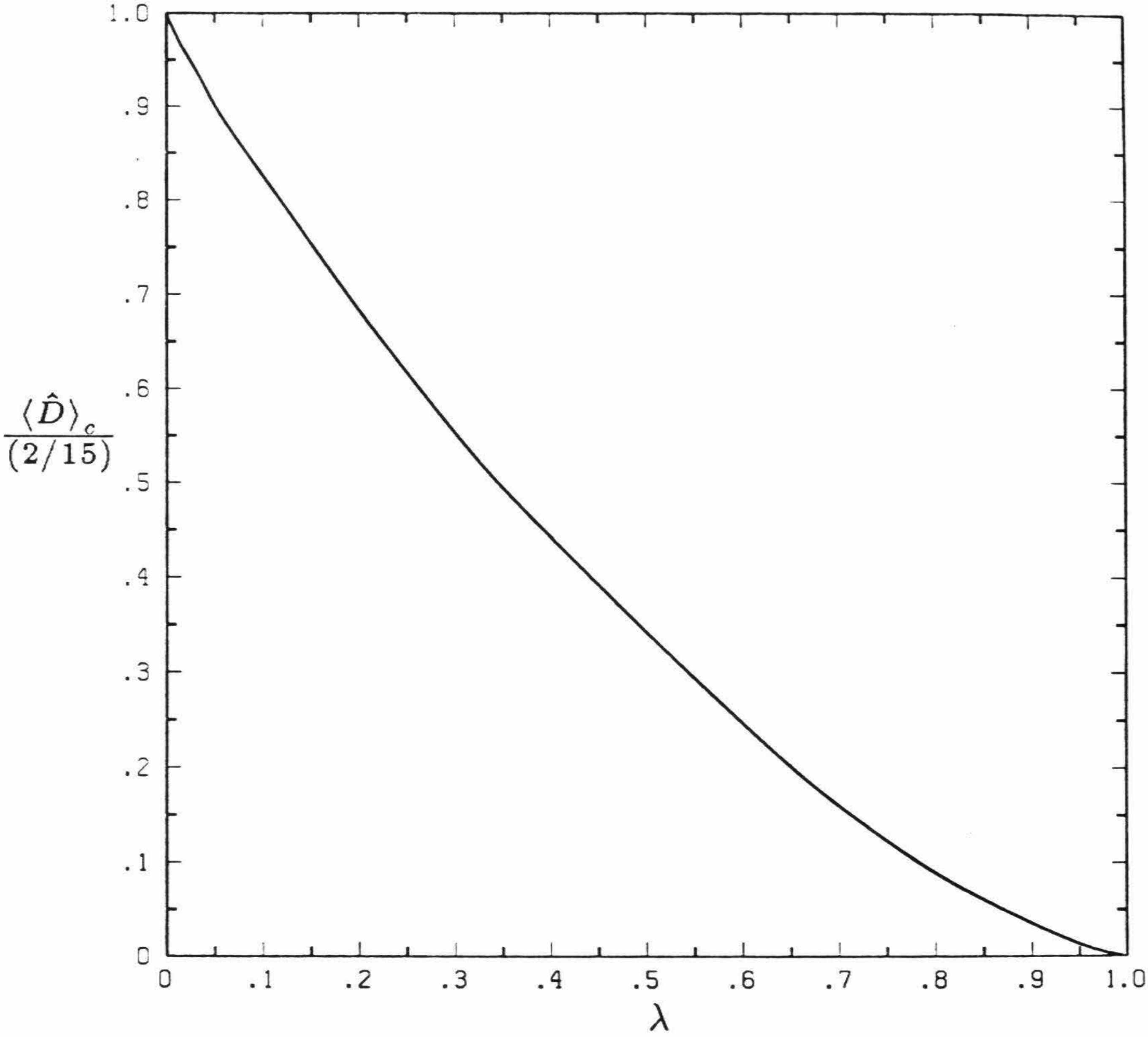

Figure 4. Effect of λ on convective dispersion coefficient.

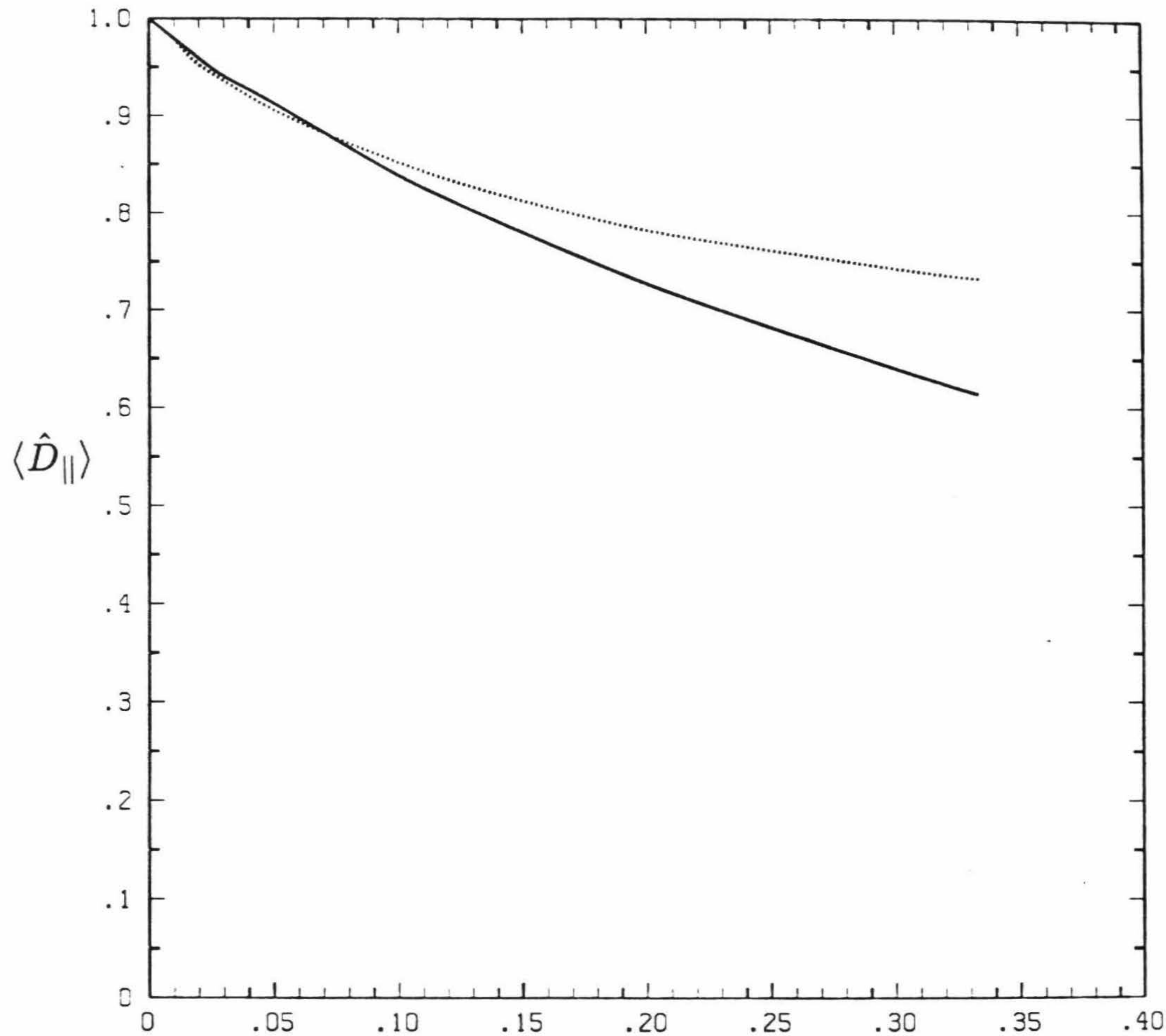

Figure 5. Comparison of numerical results and analytical solution for molecular dispersion coefficient at small λ; — numerical results, $\cdots$ analytical solution.

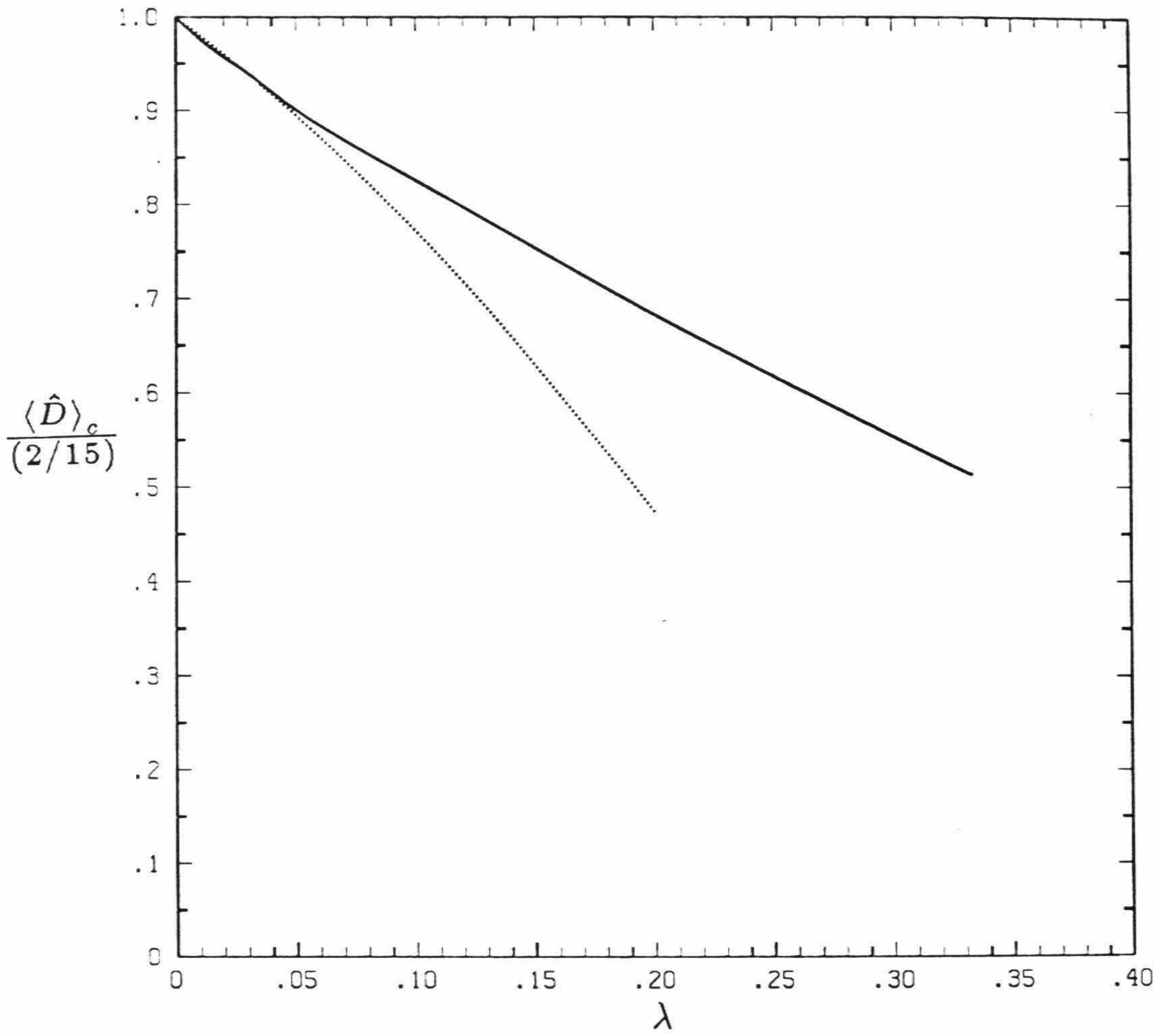

Figure 6. Comparison of numerical results and analytical solution for convective dispersion coefficient at small λ; — numerical results, $\cdots$ analytical solution.

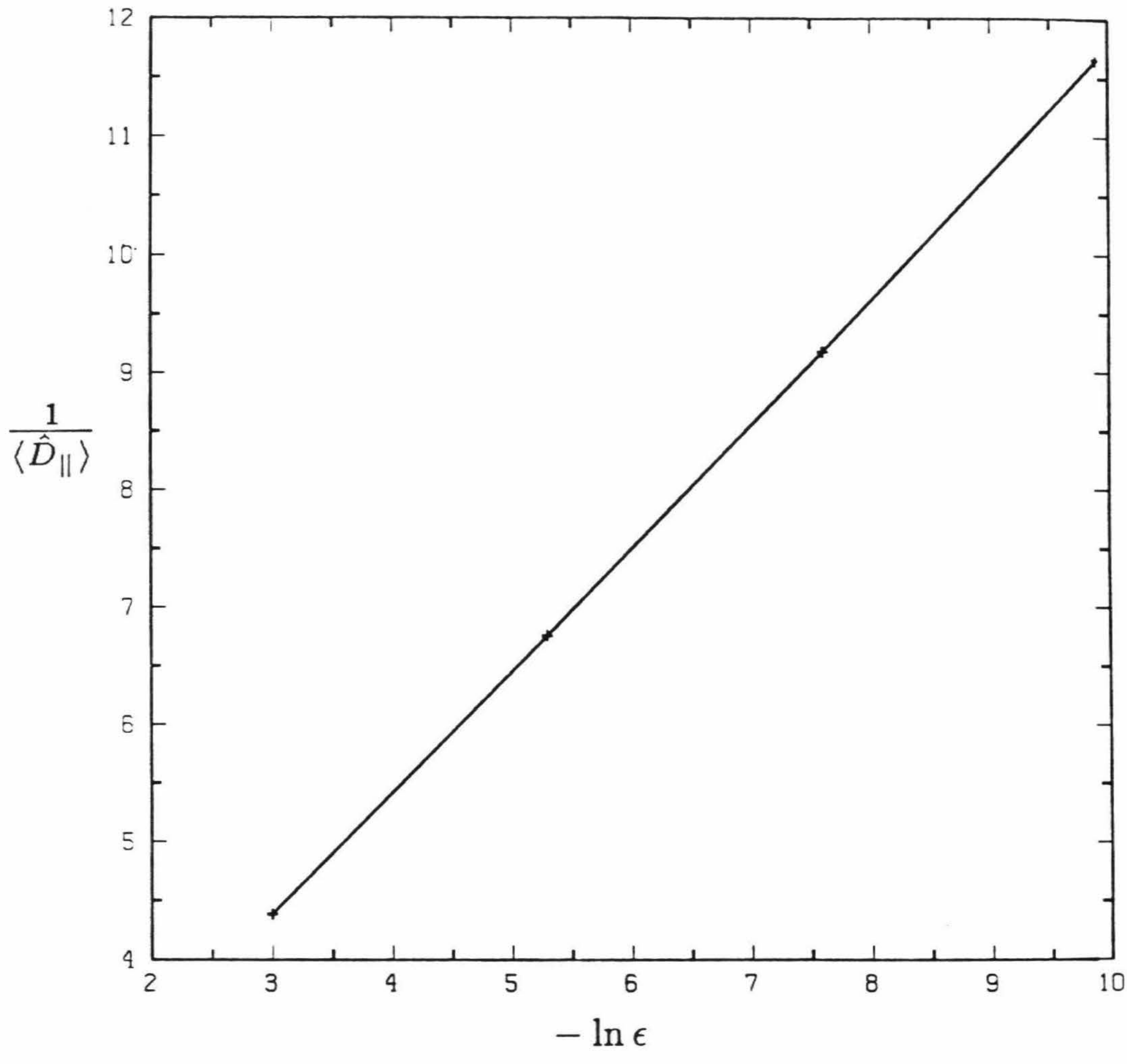

Figure 7. Dependence of $1/\langle \hat{D}_{\|} \rangle$ on $-\ln \epsilon$ for $\epsilon \ll 1$. The relationship between the two is linear, with a slope of 1.0 and intercept of 1.2.

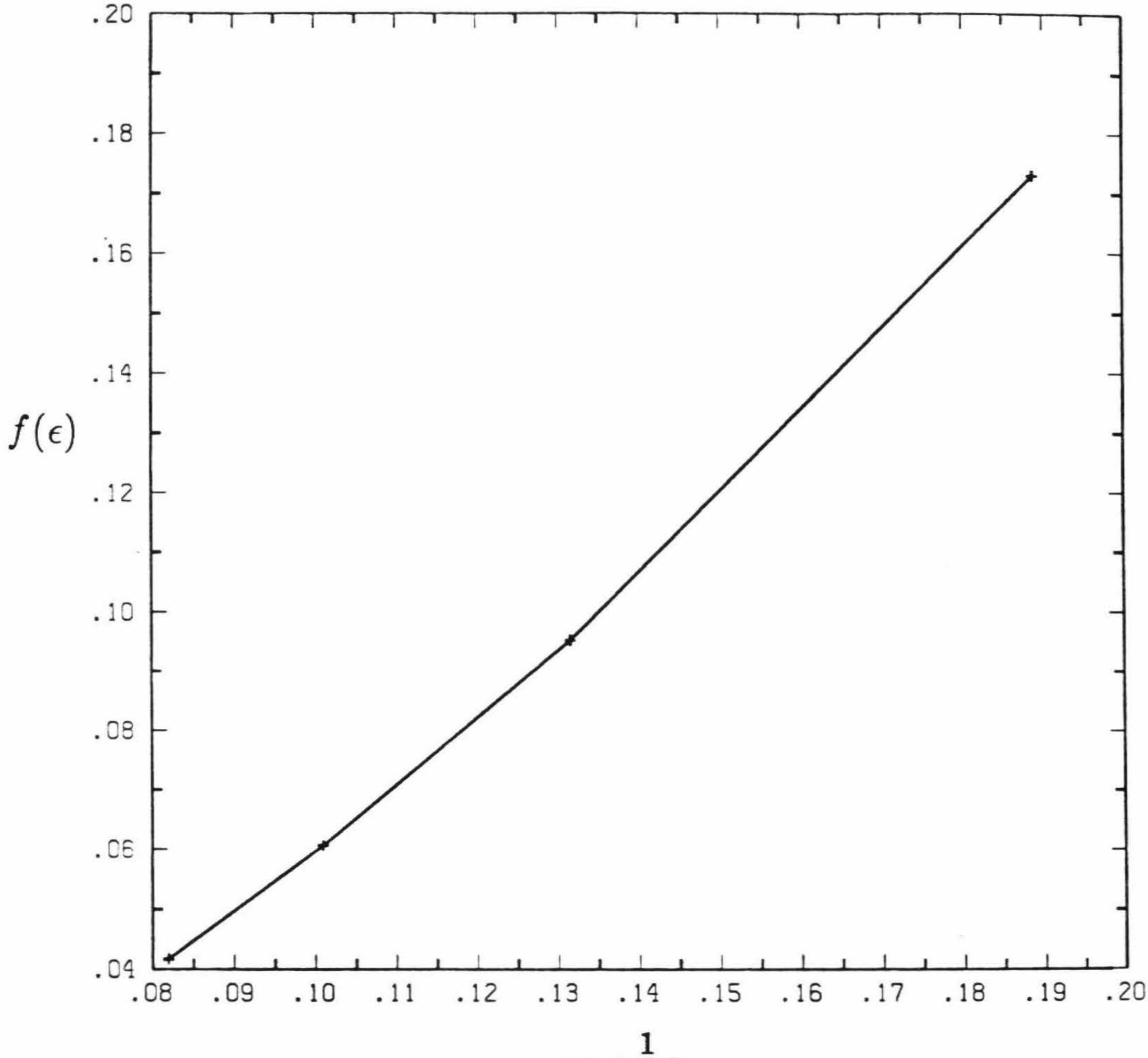

Figure 8. Dependence of $f(\epsilon)$ on $-1/\ln \epsilon$. The relationship is roughly linear.